excluding the three sections $\mathbf{u} = \mathbf{0}$, $\mathbf{v} = \mathbf{0}$ and $\mathbf{u} = \mathbf{v}$ as mentioned. Some problems, however, need further attention.

The identification of peaks in the (estimated) double Patterson function may be executed in several ways. Using more strong triplets results in more reliably identified peaks. As mentioned, all triplets may be included in the double Patterson function (10). The number of identified peaks is determined by some criterion in the identification method, such as height and sharpness of the peak. This criterion should be strengthened as more peaks are identified, leading to better estimated triplets.

When a number of peaks in the double Patterson function are identified, the corresponding triangles in the true structure may have interatomic vectors in common. By this partial overlap, the number of terms in the expression for the β_μ values, (5), decreases. In other words, a collection of triangles from the double Patterson function must be assembled into some group of interatomic vectors in order to compute the β_μ values with (5). It is not yet clear how this assembling of triangles of atoms into partially overlapping triangles can be done. It is expected that for this higher Patterson functions and higher multiplets are needed. Also, the single Patterson function may serve as an indication for this partial overlap of triangles.

Although the true double Patterson function fixes the enantiomorph, the approximated one, (11), does not do so. For this approximated double Patterson function, there are pairs of peaks $(\mathbf{u},\mathbf{v})$ and $(-\mathbf{u},-\mathbf{v})$. It may be assumed that by a choice of only one of the two peaks (and the other corresponding five peaks as mentioned above), the enantiomorph may be fixed by the first choice of the strongest non-origin peak. In the triplet expectation values computed by (8), this choice of enantiomorph will also yield triplet values in which the enantiomorph is fixed up to some accuracy; this also holds for the recomputed double Patterson function (10). From that moment on, of a pair of peaks $(\mathbf{u},\mathbf{v})$ and $(-\mathbf{u},-\mathbf{v})$, one will be larger than the other and the largest peak is, of course, to be preferred. In this way, by choice of the first strongest peak, the enantiomorph ambiguity may be solved.

The problems mentioned make application of the formulae presented to standard structure-solution methods difficult. Higher-order Patterson functions (Giacovazzo, 1980; Vaughan, 1958) may also be considered in order to solve these problems.

The author thanks Dr R. Peschar for many useful discussions.

References

COCHRAN, W. (1955). *Acta Cryst.* **8**, 473–478.

GIACOVAZZO, C. (1980). *Direct Methods in Crystallography*. London: Academic.

HAUPTMAN, H. (1976). *Acta Cryst.* A**32**, 877–882.

HAUPTMAN, H. & KARLE, J. (1962). *Acta Cryst.* **15**, 547–551.

HEINERMAN, J. J. L. (1977). *Acta Cryst.* A**33**, 100–106.

KARLE, J. (1972). *Acta Cryst.* B**28**, 3362–3369.

KRONENBURG, M. J., PESCHAR, R. & SCHENK, H. (1991). *Acta Cryst.* A**47**, 469–480.

KROON, J. & KRABBENDAM, H. (1970). *Acta Cryst.* B**26**, 312–314.

PATTERSON, A. L. (1935). *Z. Kristallogr.* **90**, 517–542.

SAYRE, D. (1953). *Acta Cryst.* **6**, 430–432.

VAUGHAN, P. A. (1958). *Acta Cryst.* **11**, 111–115.

Acta Cryst. (1993). A**49**, 877–880

Correction for the Dynamical Electron Diffraction Effect in Crystal Structure Analysis

BY SHA BING-DONG, FAN HAI-FU AND LI FANG-HUA

Institute of Physics, Chinese Academy of Sciences, Beijing 100080, *People's Republic of China*

(*Received* 19 *March* 1993; *accepted* 6 *May* 1993)

Abstract

A method is proposed to correct for the dynamical electron diffraction effect in crystal structure analysis. A rough structure model is first obtained by conventional structure-analysis methods neglecting the dynamical diffraction effect. From the rough structure model, multislice calculations are used to estimate the crystal thickness through the observed dynamical diffraction wave amplitudes. With this estimated thickness, the observed diffraction wave amplitudes are calibrated to give a set of fictitious observed kinematic structure-factor magnitudes. Based on such a set of magnitudes, a traditional least-squares procedure is used to refine structural parameters. The reliability of the result is checked by the consistency between the observed dynamical diffraction wave amplitudes and those found from

the multislice calculation. The process can be made iterative. Tests were performed with two known structures, Bi-2212 and Pb-doped Bi-2223 high-T_c superconductors, and satisfactory results were obtained.

Introduction

It is well known that the dynamical diffraction effect hinders the use of electron diffraction in crystal structure analysis. However, as pointed out by Dorset, Tivol & Turner (1992), the dynamical perturbations to the diffracted beams are first expressed as phase distortions before the wave amplitudes change much from their kinematical values. This means that in practice it is still possible to treat a set of electron diffraction data kinematically with traditional methods to obtain a rough structure. In fact, kinematic electron diffraction analysis has been successfully applied to solve a number of crystal structures, including some unknown incommensurate modulated structures (Dorset, 1993, and references therein; Xiang, Fan, Wu, Li & Pan, 1990; Mo *et al.*, 1992). On the other hand, given a structure model, it is easier to take into account the dynamical diffraction effect and apply the result to refine the structure. Dorset *et al.* (1992) showed that when a structure model is available it is possible to estimate the sample thickness through the observed dynamical diffraction data using multislice calculations. This leads to a better match between the observed and calculated structure-factor magnitudes. In this paper, it is shown that the estimated sample thickness can be used to calibrate the observed dynamical diffraction data to give a set of kinematical structure-factor magnitudes. The latter can then be used in an ordinary least-squares procedure to refine the structure model.

The method

Given a structure model and the sample thickness, one can obtain a set of dynamical diffraction wave amplitudes $|Q_c(\mathbf{H})|$ by multislice calculations (see Cowley, 1981). By changing the thickness in a wide range with small interval, say from 0 to 200 Å with intervals of 5 Å, an optimum thickness can be found that leads to the best match between the calculated, $|Q_c(\mathbf{H})|$, and the observed, $|Q_o(\mathbf{H})|$, dynamical diffraction wave amplitudes. Let $F_c(\mathbf{H})$ denote structure factors calculated from the structure model and $F_o(\mathbf{H})$ denote the *fictitious* observed structure factors, the magnitudes of which are needed for carrying out an ordinary least-squares structure refinement. Obviously, if the structure model is essentially correct, then, for each particular reflection, the relation between $|F_o(\mathbf{H})|$ and $|Q_o(\mathbf{H})|$ should be about the same as that between $|F_c(\mathbf{H})|$ and $|Q_c(\mathbf{H})|$. Hence, we can calculate approximately the value of $|F_o(\mathbf{H})|$ from

$$|F_o(\mathbf{H})|^2 - |Q_o(\mathbf{H})|^2 = |F_c(\mathbf{H})|^2 - |Q_c(\mathbf{H})|^2, \quad (1)$$

that is

$$|F_o(\mathbf{H})|^2 = |F_c(\mathbf{H})|^2 - |Q_c(\mathbf{H})|^2 + |Q_o(\mathbf{H})|^2. \quad (2)$$

With the values so obtained, the initial structure model can be refined by an ordinary least-squares procedure. The refined structure model is then used to derive a new (refined) sample thickness and to calculate new values of $|Q_c(\mathbf{H})|$ and $|F_c(\mathbf{H})|$. This leads to a new set of $|F_o(\mathbf{H})|$ from (2). New cycles of least-squares refinement can then be carried out. The whole process is summarized in Fig. 1.

Tests and results

Two known incommensurate modulated structures of high-T_c superconducting phases, Bi-2212 and Pb-doped Bi-2223, were used for the test calculations. Since the testing structures are four-dimensional periodic structures, the multislice calculation is slightly modified as described in the Appendix. On the other hand, since our method is proposed not only for use with incommensurate structures and, in the following examples, the intensities as well as the effects of dynamical diffraction of the satellite reflection are relatively weak in comparison with those of the main reflections, our test calculations were carried out with only main reflections.

1. Bi-2212 *phase* (*Fu et al.*, 1993)

The structure belongs to the superspace group N^{Bbmb}_{111} with unit-cell parameters $a = 5.40$, $b = 5.39$, $c = 30.60$ Å and modulation wave vector $\mathbf{q} = 0.21\mathbf{b}^* + \mathbf{c}^*$. Intensities of 109 $0klm$ reflections, including 31 main reflections and 78 satellites, were measured from the electron diffraction pattern taken with an H-9000 electron microscope operated at 300 kV. The incident electron beam is parallel to the a axis. The slice thickness Δx is chosen for convenience as equal to the length of the a axis, 5.40 Å. Multislice calculations were performed with different sample thicknesses ranging from 1 slice to 50 slices with an interval of 1 slice. The optimum thickness was 18

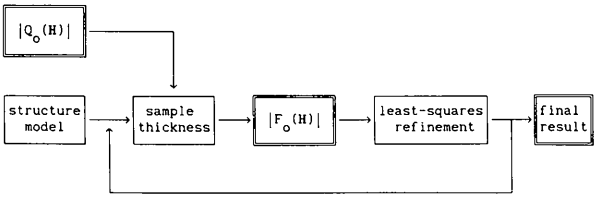

Fig. 1. Flow chart of the structure refinement procedure taking account of the dynamical diffraction effect.

Table 1. *The 20 reflections with largest differences between $|Q_o(\mathbf{H})|$ and $|F_c(\mathbf{H})|$ for* Bi-2212

					$\lvert Q_c(\mathbf{H})\rvert$			
k	l	m	$\lvert Q_o(\mathbf{H})\rvert$	$\lvert F_c(\mathbf{H})\rvert$	Cycle 0	Cycle 1	Cycle 2	Cycle 3
0	6	0	34.42	2.16	2.18	1.55	16.43	19.18
0	2	0	53.29	27.00	28.60	30.83	37.70	40.50
0	8	0	63.60	40.44	42.30	42.70	49.62	50.84
0	4	0	32.52	13.41	14.40	14.53	30.63	32.51
0	18	0	28.40	12.78	11.44	13.79	19.40	16.61
0	12	0	44.99	60.00	61.27	61.27	44.84	46.91
2	0	0	51.77	66.07	68.11	68.45	66.24	65.19
4	0	0	10.81	21.93	14.04	14.06	14.63	15.52
4	2	0	8.43	19.48	12.29	11.81	10.75	9.82
0	14	0	32.16	21.24	21.11	23.24	38.60	38.10
2	8	0	34.77	24.28	24.17	28.94	31.19	32.86
2	6	0	17.17	7.87	8.02	11.00	13.38	17.62
0	20	0	15.53	23.80	18.73	18.12	10.53	12.56
0	22	0	14.25	7.36	5.06	5.66	1.46	4.38
2	20	0	10.11	3.32	2.08	2.58	4.47	6.02
2	10	0	27.23	21.31	20.63	21.45	22.90	24.63
0	16	0	29.85	35.48	33.39	32.56	38.38	39.67
4	6	0	4.72	0.00	5.62	4.86	4.84	3.58
0	24	0	5.40	9.99	5.43	6.69	6.73	6.37
2	12	0	17.02	13.07	12.16	13.55	15.08	17.81
R factor				0.4574	0.4104	0.3755	0.2474	0.2136
Number of slices				0	18	19	20	21
Thickness (Å)				0	97.20	102.60	108.00	113.40

$$R = \sum_H |Q_o(\mathbf{H}) - kF_c(\mathbf{H})| / \sum_H |Q_o(\mathbf{H})|$$

or

$$R = \sum_H |Q_o(\mathbf{H}) - kQ_c(\mathbf{H})| / \sum_H |Q_o(\mathbf{H})|.$$

$$k = \sum_H |Q_o(\mathbf{H})F_c(\mathbf{H})| / \sum_H |F_c(\mathbf{H})|^2$$

or

$$k = \sum_H |Q_o(\mathbf{H})Q_c(\mathbf{H})| / \sum_H |Q_c(\mathbf{H})|^2.$$

Table 2. *The 20 reflections with largest differences between $|Q_o(\mathbf{H})|$ and $|F_c(\mathbf{H})|$ for* Pb-*doped* Bi-2223

					$\lvert Q_c(\mathbf{H})\rvert$	
k	l	m	$\lvert Q_o(\mathbf{H})\rvert$	$\lvert F_c(\mathbf{H})\rvert$	Cycle 0	Cycle 1
4	0	0	251.80	862.28	644.41	645.51
0	10	0	541.50	412.19	400.84	399.68
4	2	0	248.00	143.50	107.89	109.35
0	22	0	348.10	269.64	237.44	236.06
2	0	0	660.10	734.81	704.93	700.81
4	14	0	100.30	168.32	106.15	108.76
4	20	0	64.10	131.51	66.16	66.64
0	8	0	271.90	210.89	204.26	211.75
0	14	0	461.20	405.41	388.53	397.30
2	4	0	268.30	216.35	207.25	202.80
4	4	0	102.30	51.84	38.67	36.54
0	12	0	485.60	437.78	423.17	421.67
4	18	0	64.60	109.94	60.50	59.78
0	4	0	311.50	356.52	347.01	334.85
4	12	0	183.50	139.25	91.81	91.39
2	26	0	107.90	151.05	104.78	107.16
4	10	0	136.80	179.06	123.56	123.23
0	28	0	81.20	121.80	90.93	91.99
4	16	0	54.50	94.74	56.44	54.17
2	10	0	391.10	431.30	405.22	407.44
R factor				0.3391	0.2605	0.2569
Number of slices				0	13	13
Thickness (Å)				0	71.37	71.37

$$R = \sum_H |Q_o(\mathbf{H}) - kF_c(\mathbf{H})| / \sum_H |Q_o(\mathbf{H})|$$

or

$$R = \sum_H |Q_o(\mathbf{H}) - kQ_c(\mathbf{H})| / \sum_H |Q_o(\mathbf{H})|.$$

$$k = \sum_H |Q_o(\mathbf{H})F_c(\mathbf{H})| / \sum_H |F_c(\mathbf{H})|^2$$

or

$$k = \sum_H |Q_o(\mathbf{H})Q_c(\mathbf{H})| / \sum_H |Q_c(\mathbf{H})|^2.$$

slices. Table 1 lists the 20 reflections with the largest differences between $|Q_o(\mathbf{H})|$ and $|F_c(\mathbf{H})|$. The R factor,

$$R = \sum_H |Q_o(\mathbf{H})| - |F_c(\mathbf{H})| / \sum_H |Q_o(\mathbf{H}),$$

calculated with $\Delta x = 0$ and $\Delta x = 18$ slices for these 20 reflections is 0.457 and 0.410, respectively. With $\Delta x = 18$ slices, a set of $|F_o(\mathbf{H})|$ is derived from (2) and used in a least-squares structure refinement. This led to a new optimum thickness of 19 slices and a new R factor of 0.376 for the 20 reflections (see 'cycle 1' in Table 1). The procedure converged finally at a Δx value of 21 slices and an R factor of 0.214 for the 20 reflections.

2. Pb-*doped* Bi-2223 *phase* (*Mo et al.*, 1992)

The structure belongs to the superspace group P^{Bbmb}_{111} with unit-cell parameters $a = 5.49$, $b = 5.41$, $c = 37.1$ Å and modulation wave vector $\mathbf{q} = 0.117\mathbf{b}^*$. Intensities of 112 $0klm$ reflections including 42 main reflections and 70 satellites were measured from the electron diffraction pattern taken with an H-9000 electron microsope operated at 300 kV. The incident electon beam is parallel to the a axis. The slice thickness Δx is chosen as 5.49 Å. Calculation results are listed in Table 2. The final sample thickness was 13 slices. The R factor for the 20 reflections with largest differences of $|Q_o(\mathbf{H})|$ and $|Q_c(\mathbf{H})|$ decreased from 0.339 to 0.257. It should be noticed that the starting structure model used in this example has already been refined by the least-squares procedure neglecting the dynamical diffraction effect. This means that the reduction of the R factor is mainly due to the correction of the dynamical diffraction effect.

Concluding remarks

The test results show that the method is useful. It provides a simple way to take account of the dynamical electron diffraction effect in structure refinement. While the two test samples are incommensurate modulated structures, the method is applicable to ordinary structures and is easier to apply in those cases.

APPENDIX

In our treatment, it is assumed that no modulation occurs along the a axis, which is parallel to the incident electron beam. For a one-dimensional

incommensurate modulated structure, the reciprocal vector **H** of a main or satellite reflection can be expressed in three-dimensional space as

$$\mathbf{H} = h\mathbf{a}^* + k\mathbf{b}^* + l\mathbf{c}^* + m\mathbf{q}, \qquad (A1)$$

where $\mathbf{q} = \alpha\mathbf{a}^* + \beta\mathbf{b}^* + \gamma\mathbf{c}^*$ with at least one of the coefficients α, β or γ irrational. In the present case, $\mathbf{q} = \beta\mathbf{b}^* + \gamma\mathbf{c}^*$ with β irrational. The vector **H** in (*A*1) is not a vector of a three-dimensional lattice, since there is no exact periodicity in the real three-dimensional space. It is more convenient to use the multidimensional description (de Wolff, 1974) for incommensurate modulated structures. With this we can define a four-dimensional reciprocal lattice having unit vectors

$$\mathbf{b}_1 = \mathbf{a}^*, \quad \mathbf{b}_2 = \mathbf{b}^*, \quad \mathbf{b}_3 = \mathbf{c}^* \quad \text{and} \quad \mathbf{b}_4 = \mathbf{q} + \mathbf{d}. \qquad (A2)$$

Here **d** is a unit vector perpendicular to the usual three-dimensional space. A reciprocal-lattice vector in the four-dimensional space can then be written as

$$\hat{\mathbf{H}} = h\mathbf{b}_1 + k\mathbf{b}_2 + l\mathbf{b}_3 + m\mathbf{b}_4. \qquad (A3)$$

Comparison of (*A*1) and (*A*3) shows that **H** is the projection of $\hat{\mathbf{H}}$ along the direction **d** onto the three-dimensional space. In other words, the whole three-dimensional diffraction pattern from an incommensurate modulated structure may be imagined as the projection of a hypothetical four-dimensional weighted reciprocal lattice along the direction **d** onto the usual three-dimensional space. Accordingly, an incommensurate modulated structure, in our case represented as the electron potential distribution without exact periodicity, can be regarded as a hypothetical four-dimensional periodic electron potential distribution cut by a hyperplane perpendicular to **d**, *i.e.* the three-dimensional physical space. Unit vectors of the four-dimensional direct lattice are given as

$$\mathbf{a}_1 = \mathbf{a}, \quad \mathbf{a}_2 = \mathbf{b} - \beta\mathbf{d}, \quad \mathbf{a}_3 = \mathbf{c} - \gamma\mathbf{d} \quad \text{and} \quad \mathbf{a}_4 = \mathbf{d}. \qquad (A4)$$

The four-dimensional periodic electrostatic potential distribution is denoted by $\varphi(x_1, x_2, x_3, x_4)$, where x_1, x_2, x_3 and x_4 are coordinates in the four-dimensional direct space. The transmission function for a phase object with incommensurate modulation can be obtained by cutting that for the corresponding high-dimensional crystal. In the present case, the transmission function for one slice of the sample crystal is written as

$$\dot{\mathbf{C}}q(x_2, x_3, x_4) = \dot{\mathbf{C}}\exp[-i\sigma\varphi(x_2, x_3, x_4)]. \qquad (A5)$$

Here, $\dot{\mathbf{C}}$ denotes the operation of cutting a function with the three-dimensional physical space; $q(x_2, x_3, x_4)$ is the transmission function for the four-dimensional crystal; σ is an interaction term depending on the electron wavelength; $\varphi(x_2, x_3, x_4)$ is the projection of electrostatic potential distribution along the a axis. The four-dimensional Fourier transform of the transmission function is written as

$$\Omega(H) = \sum_k \sum_l \sum_m Q(H)\delta(\mathbf{H} - k\mathbf{b}^* - l\mathbf{c}^* - m\mathbf{q}), \qquad (A6)$$

where **H** is a vector in reciprocal space. When $\mathbf{H} = k\mathbf{b}^* + l\mathbf{c}^* + m\mathbf{q}$, the propagation function for the distance between two adjacent slices $P(H)$ is given by

$$P(k,l,m) = \exp\{i\pi\lambda\Delta x[(k+\beta m)^2/b^2 + (l+\gamma m)^2/c^2]\}, \qquad (A7)$$

where λ is the electron wavelength while Δx is the slice thickness. According to the conventional multi-slice method, n-beam dynamical calculations (Cowley, 1981) for a modulated structure divided into n slices can be carried out in reciprocal space as below:

$$Q_c(\mathbf{H}) = \{\Omega(\mathbf{H}) *_{n-1} [(\Omega(\mathbf{H}) * \ldots *_2 [\{\Omega(\mathbf{H}) * \times [\Omega(\mathbf{H})P(\mathbf{H})]\}_1 P(\mathbf{H})]\ldots)P(\mathbf{H})]\}_{n-1} P(\mathbf{H}), \qquad (A8)$$

where * denotes convolution. The formula is easily extended to higher-dimensional cases.

References

Cowley, J. M. (1981). *Diffraction Physics*, 2nd ed., pp. 225–247. Amsterdam: North-Holland.

Dorset, D. L. (1993). *Microsc. Soc. Am. Bull.* **23**, 99–108.

Dorset, D. L., Tivol, W. F. & Turner, J. N. (1992). *Acta Cryst.* A**48**, 562–568.

Fu, Z. Q., Huang, D. X., Li, F. H., Li, J. Q., Zhao, Z. X., Cheng, T. Z. & Fan, H. F. (1993). In preparation.

Mo, Y. D., Cheng, T. Z., Fan, H. F., Li, J. Q., Sha, B. D., Zheng, C. D., Li, F. H. & Zhao, Z. X. (1992). *Supercond. Sci. Technol.* **5**, 69–72.

Wolff, P. M. de (1974). *Acta Cryst.* A**30**, 777–785.

Xiang, S. B., Fan, H. F., Wu, X. Y., Li, F. H. & Pan, Q. (1990). *Acta Cryst.* A**46**, 929–934.